Proteomic Analysis of Exosomes from Mutant KRAS Colon Cancer Cells Identifies Intercellular Transfer of Mutant KRAS*[S]

Michelle Demory Beckler‡§, James N. Higginbotham‡, Jeffrey L. Franklin¶‖, Amy-Joan Ham‡‡, Patrick J. Halvey**‡‡, Imade E. Imasuen‡, Corbin Whitwell**, Ming Li§§, Daniel C. Liebler**‡‡, and Robert J. Coffey‡¶‖¶¶**

Activating mutations in *KRAS* occur in 30% to 40% of colorectal cancers. How mutant KRAS alters cancer cell behavior has been studied intensively, but non-cell autonomous effects of mutant KRAS are less understood. We recently reported that exosomes isolated from mutant KRAS-expressing colon cancer cells enhanced the invasiveness of recipient cells relative to exosomes purified from wild-type KRAS-expressing cells, leading us to hypothesize mutant KRAS might affect neighboring and distant cells by regulating exosome composition and behavior. Herein, we show the results of a comprehensive proteomic analysis of exosomes from parental DLD-1 cells that contain both wild-type and G13D mutant *KRAS* alleles and isogenically matched derivative cell lines, DKO-1 (mutant *KRAS* allele only) and DKs-8 (wild-type *KRAS* allele only). Mutant KRAS status dramatically affects the composition of the exosome proteome. Exosomes from mutant KRAS cells contain many tumor-promoting proteins, including KRAS, EGFR, SRC family kinases, and integrins. DKs-8 cells internalize DKO-1 exosomes, and, notably, DKO-1 exosomes transfer mutant KRAS to DKs-8 cells, leading to enhanced three-dimensional growth of these wild-type KRAS-expressing non-transformed cells. These results have important implications for non-cell autonomous effects of mutant KRAS, such as field effect and tumor progression. *Molecular & Cellular Proteomics 12: 10.1074/mcp.M112.022806, 343–355, 2013.*

K-RAS (KRAS) is a small, monomeric GTPase whose biological activity is specified by its nucleotide binding state. Multiple lines of evidence highlight the importance of KRAS in colorectal cancer (CRC).[1] For example, activating missense mutations in *KRAS*, which lock the protein into the GTP-bound state, occur in 30% to 40% of CRCs and are strongly associated with poor prognosis (1, 2). Also, mutant *KRAS* negatively predicts responsiveness to anti-EGF receptor (EGFR) therapy (3).

Early attempts to decipher the neoplastic consequences of mutant KRAS relied on overexpression studies. A drawback of these studies is their failure to simulate the genetic conditions present in human tumors, where there is often one wild-type (WT) and one mutant *KRAS* allele (1). More recently, KRAS mutant CRC cell lines have been engineered to selectively contain either the wild-type or the mutant *KRAS* allele (4), and a single mutant *Kras* allele has been activated in the intestine using genetically engineered mice (5). Detailed studies using these complementary approaches demonstrate a wide range of tumor-promoting effects of mutant KRAS (reviewed in Ref. 6). Much of what is known about mutant KRAS pertains to its ability to alter the behavior of a transformed cell in a cell autonomous manner. With the exception of increased tumor vascularity via increased tumor-derived VEGF expression (7, 8), non-cell autonomous effects of mutant KRAS have been much less studied.

Exosomes are 30- to 100-nm secreted vesicles that have emerged as a novel mode of intercellular communication (9). We recently reported that exosomes purified from conditioned medium of mutant KRAS CRC cells contained higher levels of the EGFR ligand amphiregulin (AREG) and enhanced invasiveness of recipient cancer cells relative to exosomes from isogenically matched wild-type KRAS cells (10). These results prompted us to perform a comprehensive analysis of exosomes purified from these cells. Herein, we show that mutant KRAS induces many changes in exosomal protein composition. Notably, we show that (i) KRAS is contained within exosomes, (ii) exosomes can transfer mutant KRAS to

From the ‡Department of Medicine, Vanderbilt University Medical Center, Nashville, TN 37232; §Department of Radiology, Vanderbilt University Medical Center, Nashville, TN 37232; ¶Department of Cell and Developmental Biology, Vanderbilt University Medical Center, Nashville, TN 37232; ‖Department of Veterans Affairs Medical Center, Nashville, TN 37232; **Department of Biochemistry, Vanderbilt University Medical Center, Nashville, TN 37232; ‡‡Jim Ayers Institute for Precancer Detection and Diagnosis, Vanderbilt University Medical Center, Nashville, TN 37232; §§Department of Biostatistics, Vanderbilt University Medical Center, Nashville, TN 37232

Received August 6, 2012, and in revised form, October 12, 2012
Published, MCP Papers in Press, November 15, 2012, DOI 10.1074/mcp.M112.022806

[1] The abbreviations used are: CRC, colorectal cancer; DiD, 1,1′-dioctadecyl-3,3,3′,3′-tetramethylindodicarbocyanine; EGFR, epidermal growth factor receptor; EXO, exosome; FDR, false discovery rate; MRM, multiple reaction monitoring; WCL, whole cell lysate; WT, wild-type.

cells expressing only wild-type KRAS, and (iii) mutant KRAS-containing exosomes enhance wild-type KRAS cell growth in collagen matrix and soft agar. These results have important implications for the progression of CRC tumors by providing a mechanism by which the tumor microenvironment may be influenced by non-cell autonomous signals released by mutant KRAS-expressing tumor cells.

EXPERIMENTAL PROCEDURES

Cell Culture, Reagents, and Antibodies—DKs-8, DLD-1, DKO-1 (4), and RIE-1 cells were cultured as described elsewhere (10, 11). Cells were maintained in serum-containing DMEM (Mediatech, Manassas, VA). Bovine growth serum was purchased from HyClone (Logan, UT), and all other cell culture reagents were purchased from Mediatech unless otherwise stated. Triscarboxyethylphosphine was purchased from Pierce (Rockford, IL), sequencing grade trypsin was obtained from Promega (Madison, WI), and trifluoroethanol and dithiothreitol were acquired from Acros (Geel, Belgium). Trifluoroacetic acid, ammonium bicarbonate, and urea were purchased from Fisher Scientific (Pittsburgh, PA). All other reagents were purchased from Sigma (St. Louis, MO). For a list of other reagents, see the supplemental "Experimental Procedures" section.

Exosome Isolation—Exosomes were isolated from conditioned medium of DKs-8, DLD-1, and DKO-1 cells as previously described, with slight modification (10). Briefly, cells were cultured in DMEM supplemented with 10% bovine growth serum until 80% confluent. The cells were then washed three times with PBS and cultured for 48 h in serum-free medium. The serum-free conditioned medium was removed and centrifuged for 10 min at 300 × *g* to remove cellular debris, and the resulting supernatant was then filtered through a 0.22-μm polyethersulfone filter (Nalgene, Rochester, NY) to reduce microparticle contamination. The filtrate was concentrated ~300-fold with a 100,000 molecular-weight cutoff centrifugal concentrator (Millipore). The concentrate was then subjected to high-speed centrifugation at 150,000 × *g* for 2 h. The resulting exosome-enriched pellet was resuspended in PBS containing 25 mM HEPES (pH 7.2) and washed by centrifuging again at 150,000 × *g* for 3 h. The wash steps were repeated a minimum of three times until no trace of phenol-red was detected. The resulting pellet was resuspended in PBS containing 25 mM HEPES (pH 7.2) as described previously (10), and the protein concentrations of the exosome preparations were determined with a MicroBCA kit (Pierce). The number of exosomes per microgram of protein was determined by means of nanoparticle tracking analysis (NanoSight, Wiltshire, UK) according to the manufacturer's recommendations. Analysis was performed on three independent preparations of exosomes.

Digestion and Isoelectric Focusing of Peptides—Three separate preparations of exosomes were purified, and the same protein concentration of each sample was analyzed. The samples were digested with trypsin using a trifluoroethanol (TFE) digestion procedure as described elsewhere, with minor modifications (12), and isoelectric focusing was adapted from Cargile *et al.* (13). For detailed methods of TFE digestion and isoelectric focusing of tryptic peptides, see the supplemental "Experimental Procedures" section.

Reverse Phase LC-MS/MS Analysis—LC-MS/MS analyses were performed on an LTQ-Orbitrap hybrid mass spectrometer (Thermo Electron, San Jose, CA) equipped with an Eksigent nanoLC and autosampler (Dublin, CA). Peptides were resolved on a 100 μm × 11 cm fused silica capillary column (Polymicro Technologies, LLC, Phoenix, AZ) packed with 5 μm, 300 Å Jupiter C18 (Phenomenex, Torrance, CA) using an inline 100 mm × 4 cm solid phase extraction column packed with the same C18 resin as that previously described (14). Liquid chromatography was carried out at room temperature at a flow rate of 0.6 μl min^{-1} using a gradient mixture of 0.1% (v/v) formic acid in water (solvent A) and 0.1% (v/v) formic acid in acetonitrile (solvent B). For additional details, see the supplemental "Experimental Procedures" section.

Database Searching and Statistical Analysis of Spectral Counts—The "ScanSifter" algorithm read the tandem mass spectra stored as centroided peak lists from Thermo RAW files and transcoded them to mzML files (15). For detailed analysis, see the supplemental "Experimental Procedures" section. Protein groups identified were submitted to Webgestalt for GOSlim analysis and to the Ingenuity Pathways analysis package. In order to classify protein groups, the data were sorted based on relative levels, and proteins were identified that differed by greater than 3-fold between groups and had a false discovery rate (FDR) of less than 0.05. Classifications of proteins that had significantly different levels were made based on the DAVID (http://david.abcc.ncifcrf.gov/) and Uniprot databases.

To identify any potential proteins that might differentiate cellular mutant KRAS status, we statistically evaluated the differences using our previously published approach, with some modifications (16). To calculate the rate ratio, reported spectral counts are reverse calculated using model-generated rates and provided offset numbers. The rate ratio is the ratio of the group rates expressed as the base-2 log of the ratio of the rates (16). This ratio represents the quantitative difference between the compared groups. A generalized linear mixed effect model (17) was fitted to handle exosome values expressed as count data with repeated measurements for each cell line sample; *p* values were obtained for each comparison based on a likelihood ratio test. Rate ratios were determined by comparing the expected values of the two mutant states. An FDR controlling procedure was applied to handle the multiple comparisons when testing thousands of proteins simultaneously. To test whether there was a monotone increasing trend in exosomal levels for DKs-8, DLD-1, and DKO-1 cells, a Jonckheere–Terpstra trend test was applied (18). See the supplemental "Experimental Procedures" section for additional statistical considerations.

Detection of Peptides via LC-Multiple Reaction Monitoring—DKs-8 and DKO-1 cells were grown to 80% confluence and serum starved overnight. One million cells were incubated with 100 μg of the indicated exosomes or mock treated for 1 h under constant rotation at 37 °C. Cells were then pelleted and washed three times with ice-cold PBS, and the detection of peptides was performed as described in the supplemental "Experimental Procedures" section.

LC-Multiple Reaction Monitoring—Peptide samples were analyzed in triplicate (2-μl injection volume) on a TSQ Vantage triple quadrupole mass spectrometer (Thermo-Fisher, San Jose, CA) equipped with an Eksigent nanoLC solvent delivery system (Eksigent, Dublin, CA), an autosampler, and a nanospray source. For details, see the supplemental "Experimental Procedures" section (19). Concentrations for KRAS peptides were normalized to protein input and reported as fmol/μg protein.

For the relative quantification of exosomal marker proteins, the labeled reference peptide method was used (20). Cell samples were lysed and digested prior to LC-multiple reaction monitoring (LC-MRM) analysis as described elsewhere (21). A stable isotope labeled version of the β-actin peptide GYSFTTTAER was used as an internal standard (25 fmol/μl). The integrated chromatographic peak areas for the transitions of each targeted peptide were obtained from Skyline (22), summed, and normalized to summed peak areas for the β-actin internal standard, as we have described elsewhere (20).

Biochemical Analysis—For Western blotting, DKs-8, DLD-1, and DKO-1 cells were lysed, and proteins were resolved via SDS-PAGE and Western blotted as described in the supplemental "Experimental Procedures" section. For Western blotting, 100 μg whole cell lysate (WCL) and 10 μg exosome protein (EXO) were used for CTNND1,

ITGAV, ITGB1, RAP1, and SRC; 100 μg of WCL and 30 μg of EXO were used for CTNNA, ITGA2, LYN, and KRAS; 200 μg WCL and 30 μg EXO were used for CTTN and EPHA2; 50 μg WCL and 20 μg EXO were used for ITGA6; and 50 μg WCL was used for TUBA.

Electron Microscopy—Exosomes were purified from conditioned medium of DKs-8 or DKO-1 cells, and imaging was performed as described elsewhere (10). The diameter of 100 exosomes from each of two independent exosome preparations (200 total) was determined using ImageJ software.

Flow Cytometry Internalization Assay—To determine whether exosomes are internalized, exosomes isolated from DKO-1 or DKs-8 cells were labeled with 100 μg 1,1′-dioctadecyl-3,3,3′,3′-tetramethylindodicarbocyanine (DiD)/mg EXO and washed to remove unincorporated DiD. DKO-1 or DKs-8 recipient cells were grown to 50% confluence and cultured in serum-free medium overnight. DiD-labeled exosome internalization by recipient cells was performed as previously described (10). Briefly, cells were removed from culture dishes, washed, and incubated with DiD-stained exosomes under constant rotation for the indicated times. Cells were immediately diluted into 100 vol ice-cold PBS supplemented with 10% BSA, followed by washing. The cells were analyzed via flow cytometry to determine the total fluorescence (surface-associated exosomes + internalized exosomes) and the percentage of labeled cells. The cells were then exposed to 200 mM Sudan Black in PBS supplemented with 0.5% DMSO and 5% bovine serum for 5 min at 4 °C to quench DiD fluorescence on the surface of recipient cells. Flow cytometry was repeated to determine the fluorescence of internalized exosomes.

Microscopic Internalization Assay—DKs-8 and DKO-1 exosomes were stained with the lipophilic membrane dye DiD (Invitrogen, Grand Island, NY) as described elsewhere (10). Recipient DKs-8, DKO-1, or RIE-1 cells were plated on coverslips in 24-well tissue culture dishes at a density of 5.0×10^4 cells/well. After the cells had been maintained in serum-containing medium for 24 h, the cells were washed and incubated with serum-free medium for an additional 24 h. The adherent cells were then incubated with 100 μg of DiD-stained exosomes for 30 min at 37 °C on an orbital shaker. Subsequently, the cells were washed three times with PBS, fixed in 4% paraformaldehyde for 30 min, permeabilized with 0.2% Triton-X100, incubated with AlexaFluor 488-Phalloidin (Invitrogen), and mounted on slides. Internalization was visualized on a Zeiss LSM 510 Meta confocal microscope with a 63× objective.

Three-dimensional Cell Culture—For growth in a three-dimensional collagen gel matrix (23), three layers of collagen were used in 48-well tissue culture dishes. Prior to being plated in collagen, DKs-8 and DKO-1 cells were trypsinized, syringed, and resuspended in serum-free DMEM at a concentration of 5×10^5 cells/ml. The top and bottom layers contained 150 μl/well of PureCol collagen (Advanced Biomatrix, San Diego, CA) diluted to 2 mg/ml in serum-free DMEM. The middle layer consisted of 150 μl/well of 2 mg/ml collagen in serum-free DMEM and 5×10^3 cells. Serum-free medium or serum-free medium supplemented with 50 μg of DKs-8 or DKO-1 exosomes was added. Medium was replaced twice weekly for 2 weeks. Colonies were detected by using a Gel Count imager (Oxford Optronix, Oxford, UK). Three technical replicates were performed for each of three experiments. The mean colony number for each sample was plotted ± the S.E., and statistical significance was reported as $p < 0.05$. The results for colony diameters are reported as a boxplot through their five summary statistics: sample minimum (lowest bar), lower quartile (Q1, the lower hinge), median (Q2), upper quartile (Q3, the upper hinge), and the sample maximum (highest bar). A two-sample *t* test was applied to assess the mean colony diameter difference between the samples, and statistical significance is reported as $p < 0.001$.

Soft Agar Growth—Prior to being plated in agarose, RIE-1 cells were rotated end over end with the indicated exosomes (50 μg exosomes/5.0×10^5 cells) or mock treated for 2 h at 37 °C. The cells were then plated in six-well dishes in triplicate at a density of 6.25×10^4 cells/well in 0.4% Type VII agarose (Sigma) over a hardened layer of 0.8% agarose. The cells were incubated at 37 °C in 5% CO_2 for 7 days, and colonies were counted using a Gel Count imager. Three technical replicates were performed for each of three experiments. The mean colony number for each sample was plotted ± the S.E., and statistical significance was reported as $p < 0.01$.

RESULTS

Cellular KRAS Status Affects Exosomal Protein Composition as Determined via LC-MS/MS—Our prior study showed that exosomes released by mutant KRAS-expressing CRC cells contained markedly higher levels of AREG than exosomes from their isogenically matched WT KRAS derivatives (10). We hypothesized that there might be global changes in the protein composition of exosomes based on the mutant KRAS status of the producing cell. Exosomes were purified from the serum-free conditioned medium of parental DLD-1 cells and their isogenically matched derivatives: DKO-1 (mutant *KRAS* allele only) and DKs-8 (WT allele only) cells. Serum-containing medium was not used during collection because of the known presence of exosomes in bovine serum (24). To ensure that the exosomal preparations derived from these cells were both enriched in exosomes and relatively devoid of larger extracellular vesicles, vesicles were subjected to exosomal marker and size analysis (Fig. 1). These vesicles contained the exosome-specific markers HSP70 (25), TSG101 (26), and Flotillin-1 (10), but they did not contain voltage-dependent anion channel (VDAC), a mitochondrial protein (Fig. 1*A*). Size analysis by means of transmission electron microscopy (TEM) showed that DKs-8 vesicles had a mean diameter of 59.2 nm ± 14.2 nm and DKO-1 vesicles had a mean diameter of 56.3 nm ± 17.9 nm (Fig. 1*B*). Importantly, no vesicles were larger than 140 nm. Although we cannot exclude the possibility that other types of vesicles are contained in our preparations, these results are consistent with the reported size of exosomes (9) and smaller than the reported size of microvesicles, which range in diameter from 200 nm to 1 μm (27). Combined, these results strongly support the purity of these exosome preparations. To determine the concentration of exosomes produced by each of the cell lines, nanoparticle tracking analysis was performed. The results show relatively similar numbers of vesicles per microgram of protein for DKs-8, DLD-1, and DKO-1 exosome preparations (supplemental Fig. S1*A*), suggesting that the three cells lines secrete equivalent levels of exosomes under serum-free conditions.

To determine whether protein composition was altered in exosomes derived from DLD-1, DKs-8, or DKO-1 cells, we performed a comprehensive proteomic analysis. Three biological preparations of exosomes from each line were purified via sequential differential centrifugation. Because of the low yield associated with sucrose gradient fractionation, this pro-

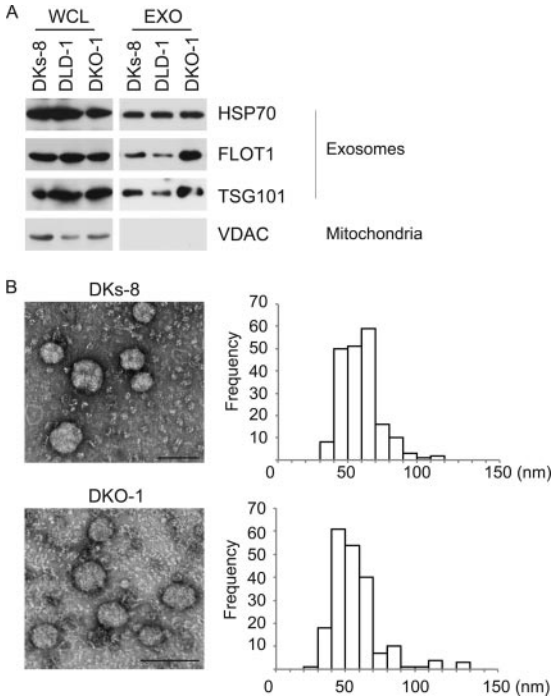

FIG. 1. **Extracellular vesicles purified from DKs-8, DLD-1, and DKO-1 cells have exosomal characteristics.** *A*, exosomes were purified from conditioned medium of DKs-8, DLD-1, and DKO-1 cells via differential centrifugation as described in the text. One hundred micrograms of whole cell lysate (WCL) protein and 10 μg of exosome (EXO) protein were resolved via SDS-PAGE and Western blotted with the indicated antibodies. Experiments were performed at least in triplicate. *B*, two independent exosome preparations from DKs-8 and DKO-1 cells were negatively stained and viewed via TEM. Representative field images show vesicles with a smooth, saucer-like morphology characteristic of exosomes (left-hand panels). The mean diameter of 200 vesicles was calculated from TEM images, and the exosome frequency was plotted for indicated size groups of 10 nm each (right-hand panels). The mean diameter for DKs-8 is 59.2 nm $\pm$ 14.2 nm, and the mean diameter of DKO-1 is 56.3 nm $\pm$ 17.9 nm. Scale bar represents 100 nm.

cedure was not used. To exclude possible microvesicle contamination, exosome preparations were filtered through a 0.22-μm filter. The purified exosomes were digested, fractionated using isoelectric focusing of the peptides, and analyzed via LC-MS/MS analysis (three technical MS replicates per sample).

LC-MS/MS datasets were searched and filtered as described earlier (see Experimental Procedures). We found a total of 185,000 confidently identified spectra corresponding to 15,359 peptides and 1,924 protein groups (minimal protein reporting with parsimony applied) (Dataset 1). This corresponded to a protein-level FDR of 2% and a peptide-to-spectrum match FDR of 0.6%. The average, standard deviation, and coefficient of variation demonstrate the high reproducibility of our analysis (supplemental Table S1). To determine the biological processes, molecular functions, and cellular components associated with the proteins identified by the LC-MS/MS analysis, GOSlim Classification analysis was used (supplemental Figs. S1*B*, S1*C*, and S1*D*). Of the 1,924 protein groups identified, 1,820 were assigned to a gene. The majority of these protein groups were shared among DKs-8, DLD-1, and DKO-1 exosomes when examined for the presence or absence of proteins (Fig. 2*A*). Twenty-three proteins were present only in DKs-8 exosomes, one in DLD-1 exosomes, and two in DKO-1 exosomes (Fig. 2*A* and Dataset 1, sheet 2). Protein groups represent protein family members that contain common tryptic peptides; hereinafter, unless otherwise stated, they are referred to as proteins.

In addition to determining the presence or absence of proteins, we also assessed the relative levels of proteins within exosomes based on donor cell mutant KRAS status. To this end, we performed both pairwise and trend analyses (Dataset 2, sheet 1, and Dataset 3). Table I represents both pairwise comparisons generated with a generalized linear mix model and Jonckheere-Terpstra (JT) trend analysis. For pairwise comparisons, all proteins represented a FDR of less than 0.05. This table represents the number of proteins whose levels were increased or decreased in the indicated exosome comparisons given rate ratio ranges of greater than 3, less than 3, but greater than 2, and less than 2, but greater than 1.5. In addition, the numbers of proteins with increasing or decreasing trends from DKs-8 to DLD-1 to DKO-1 exosomes are shown with FDR values of less than 0.05 or 0.01.

The results from a generalized linear mixed effect model of pairwise comparisons (DKs-8 *versus* DKO-1, DLD-1 *versus* DKO-1, DLD1 *versus* DKs-8) showed the greatest number of exosomal protein level differences between DKs-8 and DKO-1 exosomes (416 total proteins, Table I). Significance was defined as a greater than 3-fold difference (rate ratio) in protein level between DKs-8 and DKO-1 samples and a FDR of less than 0.05 based on pairwise analysis (Dataset 2). A heat map depicting the relative abundance of proteins with significantly different levels was generated for DKs-8 and DKO-1 exosomes. The DLD-1 exosomal protein level differences were then included in the heat map for the regulated proteins (Fig. 2*B* and supplemental Fig. S2).

Both DLD-1 cells and DKO-1 cells contain mutant KRAS. These cell lines form a similar number of tumors in nude mice and colonies in soft agar (4). Loss of WT and duplication of mutant *KRAS* alleles occurs in cancer (28–31); there is evidence that WT KRAS might act as a tumor suppressor and that the balance between mutant and WT *KRAS* alleles is critical for the oncogenic potential of KRAS. As a result, we asked whether further functional classification of exosomal proteins correlated with KRAS status in DKO-1, DLD-1, and DKs-8 exosomes. Eighty-one proteins were significantly higher in DLD-1 exosomes than in DKs-8 exosomes (Table I and Dataset 2, sheet 6); we show that proteins with fairly similar functions (endocytosis, adhesion, regulation of actin cytoskeleton) have higher levels in both DLD-1 and DKO-1 exosomes than in DKs-8 exosomes (supplemental Fig. S3).

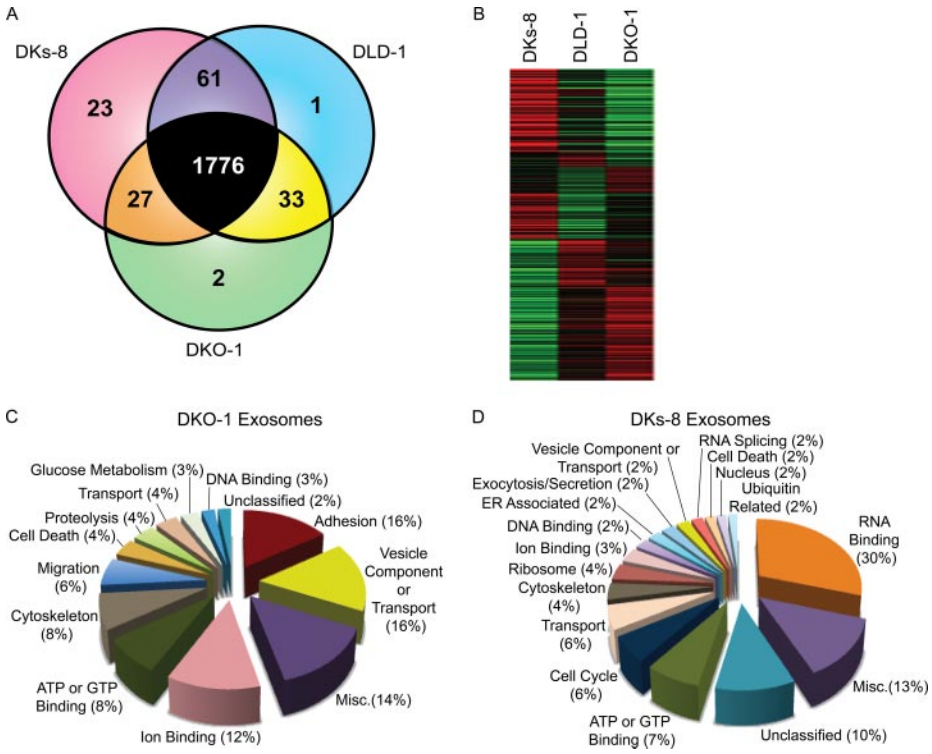

FIG. 2. **Proteomic analysis of exosomes.** *A*, Venn diagram representing the presence, absence, or overlap of protein groups identified through LC-MS/MS in the indicated exosomes. *B*, heat map representing proteins that were significantly up- and down-regulated in the DKs-8 *versus* DKO-1 pairwise analysis (see text). The data were sorted based on relative levels and proteins identified that differed by greater than 3-fold between groups and an FDR < 0.05. The DLD-1 exosomal protein level differences were included for these proteins. Red represents proteins that were up-regulated, and green represents proteins down-regulated. *C*, *D*, classification of proteins identified. Proteins that were significantly (*C*) up-regulated in DKO-1 exosomes relative to DKs-8 exosomes or (*D*) up-regulated in DKs-8 exosomes relative to DKO-1 exosomes were classified based on their Uniprot identified function. Statistical criteria used were an FDR of <0.05 and a rate ratio of >3. The results were plotted as pie charts. Classifications containing less than 2% of the total proteins were categorized as miscellaneous.

However, we chose to perform further analysis on the DKO-1 exosomes compared with the DKs-8 exosomes because this comparison yielded the greatest number of differences (Table I).

We also performed a trend analysis of protein levels in exosomes purified from the three isogenically matched cell lines using the JT trend test (Dataset 3) (18). There were 102 proteins that were increased and 276 proteins that were decreased ($p < 0.05$) based on the trend from DKs-8 to DLD-1 to DKO-1 exosomes (Table I). When more stringent criteria were applied ($p < 0.01$), 50 proteins were increased and 83 proteins were decreased.

Classification of KRAS-regulated Exosomal Proteins—Further analysis of the mutant KRAS-regulated exosomal proteins as delineated by pairwise comparison (Fig. 2*B* and supplemental Fig. S2) shows how these proteins fall into categories of distinct cellular functions. Each protein was classified by its Uniprot-defined function, and proteins within each functional group were represented as a percentage of total regulated proteins. The results were plotted as pie charts, one for proteins with levels significantly higher in DKO-1 exosomes (Fig. 2*C* and Dataset 2, sheet 2) and the other for proteins with levels significantly higher in DKs-8 exosomes (Fig. 2*D* and Dataset 2, sheet 3). Significance was defined as an FDR < 0.05 and a rate ratio of >3. Individual functional groups with lower than 2% of the total proteins were grouped and classified as miscellaneous. Proteins associated with vesicle components/transport and cellular adhesion predominated in DKO-1 exosomes, whereas RNA binding was the most heavily represented group in DKs-8 exosomes (Figs. 2*C* and 2*D*). Similar results were obtained when a more stringent FDR of <0.01 was used (data not shown). These results show that mutant KRAS expression alters exosome content by enriching exosomes with proteins involved in cellular adhesion, cytoskeletal rearrangement, and migration, processes that are often altered during cancer progression.

Confirmation of LC-MS/MS-identified Exosomal Proteins—In order to confirm the LC-MS/MS results, Western blotting analysis for specific candidate proteins was performed on DKs-8, DLD-1, and DKO-1 WCL and EXO (Fig. 3*A*). Similar to the proteomics results (Dataset 1), KRAS, EGFR, RAP1, SRC (c-Src), LYN, β1 integrin (ITGB1), α2 integrin (ITGA2), αV integrin (ITGAV), cortactin (CTTN), and p120 catenin (CTNND1) exhibited higher levels in DKO-1 exosomes than in DLD-1 and DKs-8 exosomes. In contrast, α-catenin (CTNNA) had higher levels in DKs-8 exosomes than in DLD-1 or DKO-1 exosomes. Western blotting analysis also supported the trend analysis, showing increasing levels of α6 integrin (ITGA6), β4 integrin (ITGB4), EPHA2, and EPS8 from DKs-8 to DLD-1 to DKO-1 exosomes (Figs. 3*B* and 3*C*). KRAS, CTTN, EPS8, ITGA6, ITGB4, and EPHA2 levels were significantly higher in DKO-1 than in DKs-8 exosomes, whereas CTNNA levels were significantly lower (Dataset 2 and Figs. 3*A* and 3*B*). To confirm equivalent loading, exosomal protein gels were stained with Sypro Ruby and imaged (Fig. 3*E*).

TABLE I
Proteomic and statistical appraisal of KRAS-regulated exosomal proteins based on spectral analysis

Exosome comparison	Pairwise comparison			JT trend analysis	
	Trend from DKs-8 to DLD-1 to DKO-1				
	FDR < 0.05 rate ratio			Trend *p* value FDR < 0.05	Trend *p* value FDR < 0.01
	≥3.0	<3.0, ≥2	<2, >1.5		
DKO-1 *vs.* DKs-8	↑ 126, ↓ 290	↑ 42, ↓ 82	↑ 23, ↓ 38	↑ 102, ↓ 276	↑ 50, ↓ 83
DLD-1 *vs.* DKs-8	↑ 81, ↓ 141	↑ 42, ↓ 26	↑ 18, ↓1 0		
DKO-1 *vs.* DLD-1	↑ 3, ↓ 9	↑ 3, ↓ 3	↑ 0, ↓ 3		

Pairwise comparisons in the table represent proteins with an FDR of ≤0.05. Left, the columns represent the number of proteins that had a quantitative protein level difference based on the rate ratio between the indicated exosomes. The differences are grouped as greater than or equal to 3, less than 3 but greater than or equal to 2, and less than 2 but greater than 1.5. Right, the number of proteins that exhibited an increasing trend from DKs-8 to DLD-1 to DKO-1 or a decreasing trend from DKs-8 to DLD-1 to DKO-1 based on a trend *p* value FDR of <0.05 or <0.01.

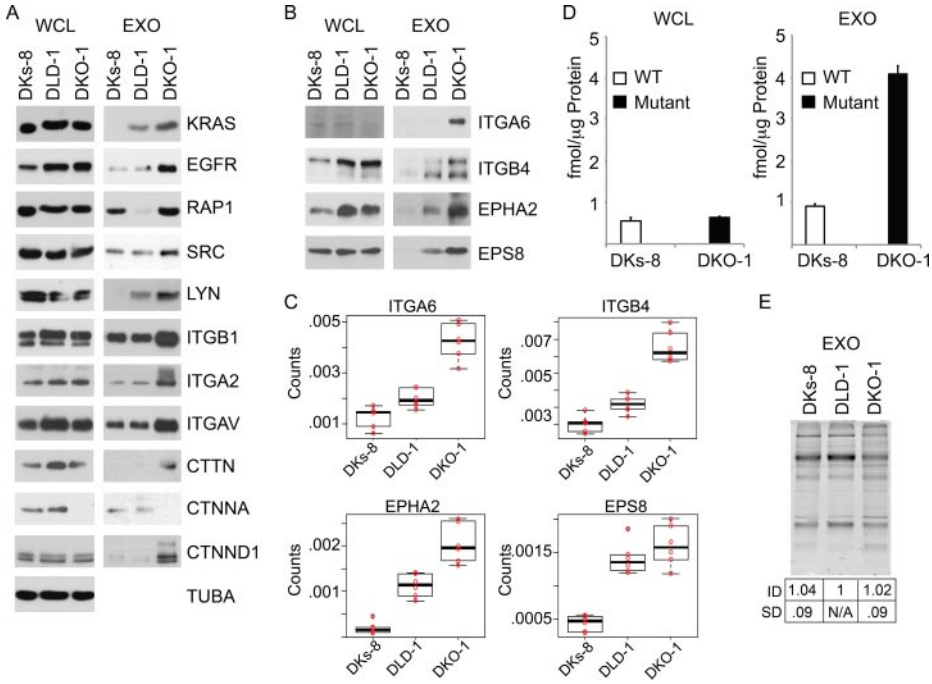

FIG. 3. **Confirmation of LC-MS/MS results.** *A*, *B*, equal concentrations of WCL and equal concentrations of EXO purified from DKs-8, DLD-1, and DKO-1 cells were resolved via SDS-PAGE and Western blotted with the indicated antibodies (for protein concentrations, see "Experimental Procedures"). *C*, trend analysis of proteins Western blotted in *B*. A trend analysis using the Jonckheere–Terpstra trend test was performed, and results for the indicated proteins were plotted. The *y*-axis indicates normalized counts, which are equivalent to the observed counts divided by the total number of confident identifications. The results follow the trend shown in *B* for ITGA6 (IPI00010697), ITGB4 (IPI00220845), EPHA2 (IPI00021267), and EPS8 (IPI00290337). *D*, KRAS is present in WCL and EXO. Proteins from DKs-8 and DKO-1 WCL and EXO (see supplemental Experimental Procedures) were resolved via SDS-PAGE and subjected to targeted LC-MRM analysis for WT (LVVVGAGGVGK) and mutant (LVVVGAGDVGK) (G13D) KRAS peptides. Concentrations of WT and mutant KRAS peptides were normalized to protein input and reported as fmol/μg protein. All experiments were performed at least in triplicate. *E*, equal protein concentrations of exosomes were resolved via SDS-PAGE and then gel stained with Sypro Ruby (see supplemental Experimental Procedures). Below, densitometry was performed on three biological replicates of DKs-8, DLD-1, and DKO-1 exosomes. Integrated densities of the entire lane were determined, and mean values (ID) and the S.D. were calculated. No statistically significant differences were found. The results show equivalent levels of exosomal proteins in the three preparations.

LC-MRM Measurement of Exosomal WT and Mutant KRAS Peptides—A notable finding was that KRAS protein was markedly enriched in exosomes from cells with mutant KRAS relative to WT KRAS only cells, despite equivalent levels of KRAS in the WCL as determined via LC-MS/MS and Western blot analysis (Fig. 3*A*, Dataset 1, Dataset 2). These methods only allow the detection of total KRAS proteins and do not distinguish between mutant and WT proteins. Therefore, to distinguish between WT and mutant KRAS, we utilized LC-MRM. Peptides specific for WT (LVVVGAGGVGK) and mutant (LVVVGAGDVGK) (G13D) KRAS were designed, and the levels of mutant and WT KRAS in DKs-8 and DKO-1 cell lines and

their respective exosomes were measured (32). In general, KRAS peptides were more abundant in exosomes than in cells. In DKs-8 exosomes, WT peptide was present at 0.9 ± 0.07 fmol/μg protein, and in cells, this value was 0.56 ± 0.07 fmol/μg protein, whereas in DKO-1 exosomes, G13D mutant peptide was present at 4.1 ± 0.19 fmol/μg protein, and in cells this value was 0.6 ± 0.02 fmol/μg protein (Fig. 3*D*). Combined, the results from LC-MS/MS, Western blotting, and targeted LC-MRM analyses strongly support the presence of WT KRAS and an enrichment of mutant KRAS in exosomes, and lead us to hypothesize that activated KRAS might have enhanced localization to exosomes.

Exosomes Are Internalized by Recipient Cells—As exosomes derived from mutant KRAS-expressing cells contain proteins involved in cancer initiation and progression, we hypothesized that internalization by recipient WT KRAS-expressing cells might alter cell behavior. To test whether exosomes are internalized, we utilized the lipophilic membrane-diffusible dye DiD to label purified exosomes and measured non-surface DiD uptake into recipient cells. Specifically, DiD-stained DKs-8 or DKO-1 exosomes were incubated with recipient DKs-8 or DKO-1 cells for 1 to 60 min. Flow cytometry was used to determine the recipient cell initial mean fluorescent DiD intensity. Cells were then incubated with Sudan Black to quench cell-surface-bound DiD-stained vesicles. Flow cytometry was repeated to quantitate the percentage of cells with internalized DiD-stained exosomes (10). The results show that greater than 80% of cells contained DiD-stained exosomes inside the cell by 5 min of incubation (Fig. 4*A*), suggesting the rapid internalization of exosomes by recipient cells.

Subsequently, we asked whether there was an increase in exosomal markers in recipient cells after a 1 h exposure to exosomes. Increased levels of the exosomal markers PDCD6IP (26), TSG101 (10, 26, 33), and CD9 (10) were detected in recipient cells via targeted LC-MRM (Fig. 4*B*). It is interesting to note that the ESCRT complex proteins PDCD6IP and TSG101 were identified in our LC-MS/MS analysis of exosomal contents (Dataset 1). Combined, these data are supportive of exosome internalization and protein incorporation by DKs-8 and DKO-1 recipient cells. Based on previous reports (34, 35), we hypothesize that exosomes might fuse with the plasma membrane and/or be internalized by recipient cells via endocytosis. Future studies will examine these possibilities.

To further examine exosome internalization, we asked whether DKs-8 and DKO-1 exosome internalization was visible by microscopy. DiD-stained DKs-8 or DKO-1 exosomes were incubated for 30 min with recipient DKs-8 cells, DKO-1 cells, or the non-transformed WT KRAS-expressing rat intestinal epithelial cell line RIE-1. The recipient cell actin cytoskeleton was visualized by means of phalloidin staining. The results show the internalization of exosomes by all recipient cells tested after 30 min of incubation (Fig. 4*C* and supplemental Fig. S4*A*). Although we cannot exclude the possibility that a population of exosomes adhere to the outside of the plasma membrane, these three pieces of data provide strong support for recipient cell internalization of exosomes.

Mutant KRAS Is Present in DKs-8 Cells after DKO-1 Exosome Incubation—Exosomes may play a role in cell–cell communication through the horizontal transfer of proteins. Having demonstrated the presence of mutant KRAS in DKO-1 exosomes (Figs. 3*A* and 3*D*) and the internalization of exosomes by recipient cells (Fig. 4), we asked whether exosomes transfer mutant KRAS to recipient cells expressing only WT KRAS. DKs-8 and DKO-1 cells were mock treated or incubated with DKs-8 or DKO-1 exosomes for 1 h, and LC-MRM was used to detect G13D and WT peptides in WCL. To account for the relative contributions to the WT peptide signal by NRAS and HRAS (LVVVGAGGVGK is common to KRAS, NRAS, and HRAS), the NRAS/HRAS-specific peptide QGVEDAFYTLVR was also monitored; it was not found to vary among the experimental conditions (Fig. 5*A*). G13D mutant peptide was detected in DKs-8 cells after incubation with DKO-1 cell-derived exosomes (0.3 ± 0.15 fmol/μg protein), suggesting the incorporation of exosome-delivered mutant KRAS protein. Corresponding increases in WT peptide after DKO-1 cells were incubated with DKs-8-derived exosomes were not observed (Fig. 5*B*). One possible explanation for this observation is that there is less WT KRAS peptide present in DKs-8 exosomes than there is $KRAS^{G13D}$ peptide in DKO-1 exosomes (Figs. 3*A* and 3*D*, Dataset 2). No other significant changes in WT or G13D peptides were observed (Fig. 5*A*). These results demonstrate a selective transfer of mutant KRAS from DKO-1 cells to DKs-8 cells via exosomes.

DKO-1 Exosomes Enhance Three-dimensional Growth of Non-transformed Cells—The ability of cancer cells to adhere to one another, survive, and proliferate while isolated within the extracellular matrix is critical to the early stages of tumor progression (36, 37). We hypothesized that exosomes purified from DKO-1 cells expressing a variety of cell adhesion, migration, cytoskeletal proteins (supplemental Fig. S1 and Fig. 2), and mutant KRAS (Figs. 3*A* and 3*D*) could, if added to DKs-8 cells, enhance their ability to grow in three dimensions. To test this possibility, DKs-8 or DKO-1 recipient cells were cultured in collagen gel with serum-free medium or serum-free medium supplemented with either DKs-8 or DKO-1 exosomes for 14 days. The results show that DKO-1 exosomes significantly increased both the number and size of DKs-8 colonies relative to serum-free control or DKs-8 exosomes (Fig. 5*C* and supplemental Fig. S4*B*). However, DKO-1 exosomes had less of an effect on DKO-1 recipient cells, likely because the same complement of proteins presented are produced.

In addition, we compared the transforming effect of DKO-1 and DKs-8 exosomes on the non-transformed WT Kras-expressing rat intestinal epithelial cell line RIE-1. The ability of cells to form anchorage-independent colonies in

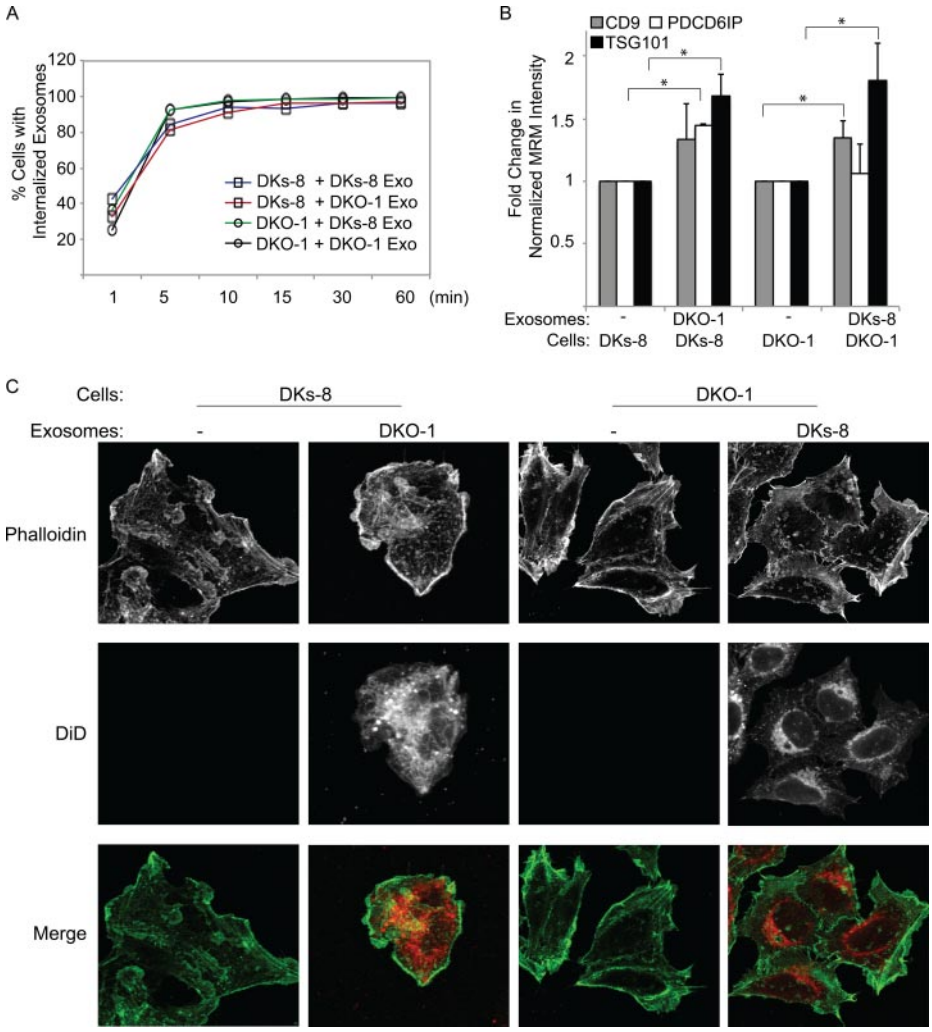

FIG. 4. **KRAS-containing exosomes are rapidly internalized.** *A*, DiD-stained exosomes were purified from DKs-8 and DKO-1 cells and incubated with recipient DKs-8 or DKO-1 cells for the indicated times. Flow cytometric analysis was performed as described in the text. Ten thousand events were counted, and the experiment was performed in triplicate. *B*, exosomal markers increase in recipient cells after incubation with exosomes. Recipient cells were incubated with the indicated exosomes for 1 h, and cell extracts were subjected to targeted LC-MRM analysis. The chromatographic peak areas for the transitions of each targeted peptide were summed, normalized to summed peak areas for the β-actin internal standard, and plotted as the fold change in the normalized MRM intensity $\pm$ the S.D. (* indicates a p value of <0.05). *C*, DKs-8 or DKO-1 cells were mock treated or incubated with the indicated DiD-stained exosomes for 30 min. Cells were fixed, permeablized, stained with Alexa Fluor 488-phalloidin, mounted, and visualized by means of confocal microscopy.

soft agar is a hallmark of the transformed phenotype. RIE-1 cells were plated in soft agar with mock treatment, DKs-8 exosomes, or DKO-1 exosomes. After 7 days, colony formation was measured; the results showed a statistically greater number of colonies when cells were co-incubated with DKO-1 exosomes than when incubated with DKs-8 exosomes (Fig. 5*D*), further supporting the idea that mutant KRAS-containing exosomes enhance the transformation of non-transformed WT KRAS-expressing cells. Taken together, these results strongly suggest that altering the KRAS status within a cell significantly alters its exosome proteome and the functional consequences of these exosomes for recipient cells.

DISCUSSION

Exosomes are implicated in intercellular signaling and as regulators of tumor progression; however, it is unknown the extent to which the contents of exosomes differ between normal and cancer cells and how signals transmitted by exosomes might vary. To examine whether KRAS status affected exosome composition and behavior, we purified exosomes from DLD-1 (mutant and WT KRAS) cells and its KRAS variant isogenic cell lines: DKs-8 (WT KRAS only) and DKO-1 (mutant KRAS only). A comprehensive proteomic analysis was performed, and the results show that KRAS status markedly affects exosome composition (Dataset 1). Exosomes purified from cells expressing mutant KRAS contain higher levels of

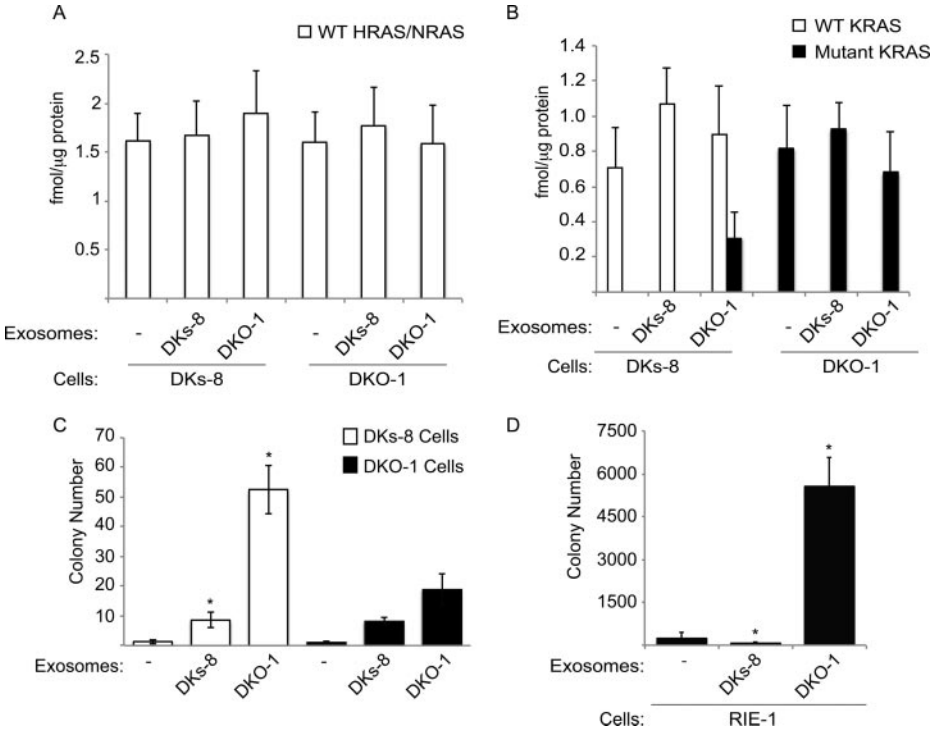

FIG. 5. **DKO-1 exosomes transfer mutant KRAS to DKs-8 cells and enhance three-dimensional growth of non-transformed cells.** *A*, *B*, mutant (G13D) KRAS is present in DKs-8 cells after incubation with DKO-1 exosomes, whereas WT HRAS and NRAS levels are unchanged. Concentrations of KRAS, HRAS, and NRAS peptides were normalized to protein input and reported as fmol/μg protein. Data are plotted as the mean $\pm$ S.D. Experiments were performed in triplicate. The level of G13D mutant KRAS peptide in DKs-8 cells treated with DKO-1 exosomes represents a p value of 0.00009 compared to mock treated DKs-8 control cells. *C*, DKs-8 and DKO-1 cells were plated in collagen matrix as described in the text. The cells were cultured in serum-free medium or serum-free medium supplemented with the indicated exosomes for 14 days, and the respective media were changed twice weekly. Three independent experiments were performed in triplicate. The colony number was quantified and plotted. Data represent the mean $\pm$ the S.E. (* indicates $p < 0.05$). *D*, RIE-1 cells were plated in soft agar with mock treatment, DKO-1 exosomes, or DKs-8 exosomes and cultured for 7 days. Colonies were counted and plotted as the mean $\pm$ the S.E. (* indicates $p < 0.01$). Three independent experiments were performed in triplicate.

cancer-associated proteins than do exosomes from cells expressing only WT KRAS (Figs. 2, 3*A*, and 3*B*; supplemental Fig. S1). Among these proteins is KRAS itself (Fig. 3*A*). We have shown that mutant KRAS is enriched relative to WT KRAS in exosomes (Fig. 3*D*). Further, we have shown that mutant KRAS-containing exosomes purified from DKO-1 cells transfer mutant KRAS to recipient DKs-8 cells that express only WT KRAS (Fig. 5*B*). Exosomes are rapidly internalized by DKs-8 recipient cells (Figs. 4*A*–4*C*), and DKs-8 cells have significantly enhanced growth in three dimensions in response to exosomes containing mutant KRAS (Figs. 5*C* and 5*D*; supplemental Fig. S4*B*). Combined, our results suggest that the mutation of KRAS can alter the signals released by cells via exosomes, leading to a growth advantage for nearby WT KRAS-containing cells.

Our study is the first to specifically detect KRAS in exosomes (Figs. 3*A* and 3*D*, Datasets 1 and 2). Ras family members have been detected in a variety of vesicles. KRAS associates with early endosomes, late endosomes, and lysosomes, as well as recycling endosomes (38); KRAS and HRAS bind to Arf6-associated clathrin-independent endosomes (38). HRAS and NRAS, but not KRAS, are reported to localize in ~100-nm non-plasma membrane-derived cytoplasmic vesicles termed rasosomes (39, 40).

HRAS and NRAS have been found in exosomes purified from transformed cells (41, 42) and urine (43). HRAS, NRAS, and KRAS were previously detected in exosomes via LC-MS/MS; however, that study did not describe the peptides identified, and further validation was not provided (44). Therefore, we are the first to document the presence of KRAS in exosomes, not only by means of LC-MS/MS proteomics, but also through targeted LC-MRM and Western blot analysis (Figs. 3*A*, 3*D*; Datasets 1 and 2). Moreover, we show that the level of KRAS in exosomes increases when mutant KRAS is expressed in the donor cell (Figs. 3*A*, 3*D*; Datasets 1 and 2), suggesting that mutant KRAS localizes to exosomes to a greater extent than WT KRAS, which might be a process directly or indirectly regulated by activated mutant KRAS itself.

Although we do not know the mechanism(s) by which KRAS traffics to exosomes or why mutant KRAS is preferentially targeted there, we propose several possibilities: plasma membrane aggregated active KRAS might induce trafficking to exosomes; localization might be enhanced by protein mod-

ification of KRAS, such as protein kinase C phosphorylation of the KRAS hypervariable region, leading to its accumulation at endomembranes (45); KRAS might "piggy-back" with binding partners that are targeted to exosomes, particularly those binding partners that interact with GTP-bound KRAS; and finally, in our favored model, ubiquitin modification of KRAS regulates its trafficking to exosomes.

A recent report shows that KRAS is ubiquitylated (46). Because ubiquitylation has been implicated in exosomal sorting (47), and given that ubiquitin is one of the most abundant peptides based on the number of spectra detected by proteomics in our exosomes (Dataset 1), ubiquitin-modified activated KRAS might be specifically targeted to these vesicles. This hypothesis is supported by the concordance of identified protein groups in our exosomes with those found in the ubiquitin-modified proteome of HCT116 cells (48). This corresponds to a 58% overlap of the exosomal identified proteins (Dataset 1) with the identified ubiquitin-modified proteins (p value of <0.001) (Dataset 4) when using Fisher's exact test for the null hypothesis of independence of these two studies. If we estimate the lower limit of the number of proteins per cell as ~10,000 (supplemental Experimental Procedures), then our analysis excludes the random association of exosome proteins with ubiquitin-modified proteins. The significance of this overlap indicates that this is a non-random association (49). Future investigations will examine how KRAS is trafficked to exosomes and whether ubiquitin modification regulates KRAS and other proteins trafficking to exosomes.

Exosomal proteomic analysis shows other KRAS-induced differences that might have non-cell autonomous functional consequences. Integrins are one such class of proteins that might facilitate exosome-induced effects on cell adhesion (50), migration (51), or invasion (10). Many of the identified integrin subunits (ITGB1, ITGA2, ITGAV, ITGA6, and ITGB4) (Dataset 1) were previously reported as exosomal components (52), but we have shown that their exosomal composition is regulated by mutant KRAS. This observation is supported by earlier reports showing the regulation of integrin expression or activity by KRAS. Decreased expression of ITGB1 has been detected in cancer tissue (53), and the expression of G12V mutant KRAS in HD6–4 colon cancer cells inhibits ITGB1 glycosylation and loss of cell–cell adhesion (54). Induced expression of the ITGAV subunit increases the metastatic potential of melanoma cells (55), and its levels are decreased upon antisense knockdown of mutant KRAS in SW480 cells (56), supporting the notion that KRAS regulates its expression. Similarly, ITGA6–ITGB4 complex expression is up-regulated in a number of cancers, and its induction correlates with progression to invasive carcinoma (55). Keratinocytes lacking the ITGA6–ITGB4 complex are resistant to Ras transformation, suggesting a cooperative role of these proteins in cancer progression (57). Combined, these reports support the idea that integrin subunits and complexes are regulated by and cooperate with Ras to promote tumor aggressiveness. Future studies will determine whether the presence of integrin subunits or complexes in exosomes also plays a role in this phenomenon.

A number of proteins with higher levels in DKO-1 exosomes have been found in tumor-adjacent tissue, including mutant KRAS, EGFR, and SRC (58), suggesting that aberrant expression of these proteins predisposes tissue to cancer growth, and the introduction of other proteins contained in exosomes also might provide a growth advantage. Among these, EPHA2 and EPS8 levels positively correlate with mutant KRAS expression in cancer tissue and cells (59, 60), and when KRAS is transfected into intestinal epithelial cells, enhanced CTNND1 phosphorylation is observed (61). These proteins might play an important role in imparting exosome-induced effects on recipient cells. Further, several of the most significantly mutated genes detected in CRC (62) (KRAS, NF1, ARID1A, MSH2, CTTNB1, and PIK3R1) were found in the DKO-1 exosomes, making exosomal delivery of mutant forms of these proteins to adjacent tissue a potential mechanism by which tumors may promote field effect.

Field effect has been proposed to explain how histologically non-dysplastic epithelium is preconditioned for cancer growth (63), and it appears to result from growth advantages provided by the tumor microenvironment. Because KRAS is often mutated in colon cancer cells and tissues (64), and because this dysregulates a variety of intracellular signaling processes (65), it is important to determine the contribution of KRAS to field effect. The observed non-cell autonomous effects induced by mutant KRAS-containing exosomes (Fig. 5) suggest that exosomes might play a role in mutant KRAS-induced field effect and the establishment of the tumor niche.

We hypothesize that one mechanism by which mutant KRAS-containing exosomes might facilitate tumor niche development is alteration of the tumor stroma. Recently, active Wnt proteins were found to be localized in exosomes, and these exosomes activate the transcription of an exogenously expressed Wnt reporter in recipient cells (66). Peinado *et al.* showed that bone marrow from mice exposed to melanoma-derived exosomes induced greater primary tumor size and numbers of metastases than bone marrow from control mice (67). Additionally, it has been reported that cancer-derived exosomes enhance fibroblast-to-myofibroblast differentiation (68). Given these reports, one of our future directions is to begin analyzing whether mutant KRAS-containing exosomes similarly alter the tumor microenvironment. We cannot exclude the possibility that exosomes from normal cells surrounding the tumor niche also might have a suppressive effect in tumor growth.

In addition to exosomes exerting field effects on local cells, exosomes may also induce non-cell autonomous effects at distant metastatic sites. When Paget first asserted the "seed and soil" hypothesis (69), it was unknown what factors might

enrich a distant site, making it hospitable for metastatic growth. More recently, Kaplan *et al.* found that conditioned medium purified from Lewis lung carcinoma cells or B16 melanoma cells stimulated the migration of VEGFR1$^+$ bone-marrow-derived cells (BMDC) through Transwell filters to a greater extent than serum-containing medium. Further, this study showed that the intraperitoneal injection of cancer cell-conditioned medium could direct the formation of metastatic deposits of injected cancer cells *in vivo* (70). The authors hypothesize that chemokines or cytokines present in the conditioned medium of cancer cells are responsible for the metastatic growth of BMDC; however, given our results of exosomal transfer of mutant KRAS (Fig. 5*B*) and enhanced three-dimensional growth of WT KRAS cells stimulated by mutant KRAS-containing exosomes (Figs. 5*C* and 5*D*; supplemental Fig. S4*B*), it is possible that exosomes play a key role in a similar phenomenon in colon cancer.

The study of exosomes in cancer is a nascent field of inquiry, and many questions remain unanswered. Among these are how proteins are targeted to exosomes, what the mechanism of exosome biogenesis and uptake is, how exosomes exert effects on recipient cells, and how cancer cells exploit exosomal content transfer or signaling to enhance the tumor microenvironment. This study sheds light on several of these questions by providing evidence that donor cell mutant KRAS expression alters exosome content, allowing for exosomal localization of mutant KRAS, as well as other proneoplastic proteins; that these exosomal proteins can be transferred to recipient cells; and that mutant KRAS-containing exosomes stimulate enhanced growth of non-transformed WT KRAS-expressing cells in three dimensions. We hypothesize that these events allow mutant KRAS-expressing tumor cells to alter neighboring cells through field effect and promote metastatic progression by seeding the soil of pre metastatic niches.

Acknowledgments—We acknowledge Melissa Chambers for technical assistance, as well as Melanie Ohi and the Vanderbilt University Center for Structural Biology for use of the TEM. We also acknowledge Emily J. Poulin for editorial assistance.

* This work was supported by NCI CA46413 and GI Special Program of Research Excellence P50 95103 to R.J.C., 2R25 CA092043 to M.D.B., P30 DK058404 to J.L.F., and U24CA159988 and U01CA152647 to D.C.L. The Vanderbilt University Flow Cytometry Shared Resource is supported by the Vanderbilt Ingram Cancer Center (P30 CA68485) and the Vanderbilt Digestive Disease Research Center (P30 DK058404). Additionally, we acknowledge the Vanderbilt cell imaging, flow cytometry, proteomics, and novel cell line development cores of the DDRC (P30 DK58404).

S This article contains supplemental material.

¶¶ To whom correspondence should be addressed: Robert J. Coffey, MD, Epithelial Biology Center, 10415 MRB IV, Vanderbilt University Medical Center, 2213 Garland Ave., Nashville, TN 37232, Fax: (615) 343-1591, E-mail: robert.coffey@vanderbilt.edu.

REFERENCES

1. Pylayeva-Gupta, Y., Grabocka, E., and Bar-Sagi, D. (2011) RAS oncogenes: weaving a tumorigenic web. *Nat. Rev. Cancer* **11,** 761–774
2. Cox, A. D., and Der, C. J. (2010) Ras history: the saga continues. *Small GTPases* **1,** 2–27
3. De Roock, W., Piessevaux, H., De Schutter, J., Janssens, M., De Hertogh, G., Personeni, N., Biesmans, B., Van Laethem, J. L., Peeters, M., Humblet, Y., Van Cutsem, E., and Tejpar, S. (2008) KRAS wild-type state predicts survival and is associated to early radiological response in metastatic colorectal cancer treated with cetuximab. *Ann. Oncol.* **19,** 508–515
4. Shirasawa, S., Furuse, M., Yokoyama, N., and Sasazuki, T. (1993) Altered growth of human colon cancer cell lines disrupted at activated Ki-ras. *Science* **260,** 85–88
5. Haigis, K. M., Kendall, K. R., Wang, Y., Cheung, A., Haigis, M. C., Glickman, J. N., Niwa-Kawakita, M., Sweet-Cordero, A., Sebolt-Leopold, J., Shannon, K. M., Settleman, J., Giovannini, M., and Jacks, T. (2008) Differential effects of oncogenic K-Ras and N-Ras on proliferation, differentiation and tumor progression in the colon. *Nat. Genet.* **40,** 600–608
6. Velho, S., and Haigis, K. M. (2011) Regulation of homeostasis and oncogenesis in the intestinal epithelium by Ras. *Exp. Cell Res.* **317,** 2732–2739
7. Okada, F., Rak, J. W., Croix, B. S., Lieubeau, B., Kaya, M., Roncari, L., Shirasawa, S., Sasazuki, T., and Kerbel, R. S. (1998) Impact of oncogenes in tumor angiogenesis: mutant K-ras up-regulation of vascular endothelial growth factor/vascular permeability factor is necessary, but not sufficient for tumorigenicity of human colorectal carcinoma cells. *Proc. Natl. Acad. Sci..* **95,** 3609–3614
8. Mazure, N. M., Chen, E. Y., Yeh, P., Laderoute, K. R., and Giaccia, A. J. (1996) Oncogenic transformation and hypoxia synergistically act to modulate vascular endothelial growth factor expression. *Cancer Res.* **56,** 3436–3440
9. Schorey, J. S., and Bhatnagar, S. (2008) Exosome function: from tumor immunology to pathogen biology. *Traffic* **9,** 871–881
10. Higginbotham, J. N., Demory Beckler, M., Gephart, J. D., Franklin, J. L., Bogatcheva, G., Kremers, G. J., Piston, D. W., Ayers, G. D., McConnell, R. E., Tyska, M. J., and Coffey, R. J. (2011) Amphiregulin exosomes increase cancer cell invasion. *Curr. Biol.* **21,** 779–786
11. Barnard, J. A., Graves-Deal, R., Pittelkow, M. R., DuBois, R., Cook, P., Ramsey, G. W., Bishop, P. R., Damstrup, L., and Coffey, R. J. (1994) Auto- and cross-induction within the mammalian epidermal growth factor-related peptide family. *J. Biol. Chem.* **269,** 22817–22822
12. Wang, Y., Wang, H., Gao, L., Liu, H., Lu, Z., and He, N. (2005) Polyacrylamide gel film immobilized molecular beacon array for single nucleotide mismatch detection. *J. Nanosci. Nanotechnol.* **5,** 653–658
13. Cargile, B. J., Sevinsky, J. R., Essader, A. S., Stephenson, J. L., Jr., and Bundy, J. L. (2005) Immobilized pH gradient isoelectric focusing as a first-dimension separation in shotgun proteomics. *J. Biomol. Tech.* **16,** 181–189
14. Licklider, L. J., Thoreen, C. C., Peng, J., and Gygi, S. P. (2002) Automation of nanoscale microcapillary liquid chromatography-tandem mass spectrometry with a vented column. *Anal. Chem.* **74,** 3076–3083
15. Ma, Z. Q., Tabb, D. L., Burden, J., Chambers, M. C., Cox, M. B., Cantrell, M. J., Ham, A. J., Litton, M. D., Oreto, M. R., Schultz, W. C., Sobecki, S. M., Tsui, T. Y., Wernke, G. R., and Liebler, D. C. (2011) Supporting tool suite for production proteomics. *Bioinformatics* **27,** 3214–3215
16. Li, M., Gray, W., Zhang, H., Chung, C. H., Billheimer, D., Yarbrough, W. G., Liebler, D. C., Shyr, Y., and Slebos, R. J. (2010) Comparative shotgun proteomics using spectral count data and quasi-likelihood modeling. *J. Proteome Res.* **9,** 4295–4305
17. Faraway, J. J. (2006) *Extending the Linear Model with R: Generalized Linear, Mixed Effects and Nonparametric Regression Models*, Chapman & Hall/CRC, Boca Raton, FL
18. Jonckheere, A. R. (1954) A distribution-free k-sample test against ordered alternatives. *Biometrika* **41,** 133–145
19. Halvey, P. J., Ferrone, C. R., and Liebler, D. C. (2012) GeLC-MRM quantitation of mutant KRAS oncoprotein in complex biological samples. *J. Proteome Res.* **11,** 3908–3913
20. Zhang, H., Liu, Q., Zimmerman, L. J., Ham, A. J., Slebos, R. J., Rahman, J., Kikuchi, T., Massion, P. P., Carbone, D. P., Billheimer, D., and Liebler, D. C. (2011) Methods for peptide and protein quantitation by liquid

chromatography-multiple reaction monitoring mass spectrometry. *Mol. Cell. Proteomics* **10,** M110.006593
21. Halvey, P. J., Zhang, B., Coffey, R. J., Liebler, D. C., and Slebos, R. J. (2012) Proteomic consequences of a single gene mutation in a colorectal cancer model. *J. Proteome Res.* **11,** 1184–1195
22. MacLean, B., Tomazela, D. M., Shulman, N., Chambers, M., Finney, G. L., Frewen, B., Kern, R., Tabb, D. L., Liebler, D. C., and MacCoss, M. J. (2010) Skyline: an open source document editor for creating and analyzing targeted proteomics experiments. *Bioinformatics* **26,** 966–968
23. Chung, E., Graves-Deal, R., Franklin, J. L., and Coffey, R. J. (2005) Differential effects of amphiregulin and TGF-alpha on the morphology of MDCK cells. *Exp. Cell Res.* **309,** 149–160
24. Thery, C., Amigorena, S., Raposo, G., and Clayton, A. (2006) Isolation and characterization of exosomes from cell culture supernatants and biological fluids, in *Current Protocols in Cell Biology* (Bonifacino, J. S., *et al.*, eds.), Unit 3.22
25. Zhan, R., Leng, X., Liu, X., Wang, X., Gong, J., Yan, L., Wang, L., Wang, Y., Wang, X., and Qian, L. J. (2009) Heat shock protein 70 is secreted from endothelial cells by a non-classical pathway involving exosomes. *Biochem. Biophys. Res. Commun.* **387,** 229–233
26. Thery, C., Boussac, M., Veron, P., Ricciardi-Castagnoli, P., Raposo, G., Garin, J., and Amigorena, S. (2001) Proteomic analysis of dendritic cell-derived exosomes: a secreted subcellular compartment distinct from apoptotic vesicles. *J. Immunol.* **166,** 7309–7318
27. Cocucci, E., Racchetti, G., and Meldolesi, J. (2009) Shedding microvesicles: artefacts no more. *Trends Cell Biol.* **19,** 43–51
28. Hartman, D. J., Davison, J. M., Foxwell, T. J., Nikiforova, M. N., and Chiosea, S. I. (2012) Mutant allele-specific imbalance modulates prognostic impact of KRAS mutations in colorectal adenocarcinoma and is associated with worse overall survival. *Int. J. Cancer* **131,** 1810–1817
29. Li, J., Zhang, Z., Dai, Z., Plass, C., Morrison, C., Wang, Y., Wiest, J. S., Anderson, M. W., and You, M. (2003) LOH of chromosome 12p correlates with Kras2 mutation in non-small cell lung cancer. *Oncogene* **22,** 1243–1246
30. Soh, J., Okumura, N., Lockwood, W. W., Yamamoto, H., Shigematsu, H., Zhang, W., Chari, R., Shames, D. S., Tang, X., MacAulay, C., Varella-Garcia, M., Vooder, T., Wistuba, I. I., Lam, S., Brekken, R., Toyooka, S., Minna, J. D., Lam, W. L., and Gazdar, A. F. (2009) Oncogene mutations, copy number gains and mutant allele specific imbalance (MASI) frequently occur together in tumor cells. *PloS One* **4,** e7464
31. Zhang, Z., Wang, Y., Vikis, H. G., Johnson, L., Liu, G., Li, J., Anderson, M. W., Sills, R. C., Hong, H. L., Devereux, T. R., Jacks, T., Guan, K. L., and You, M. (2001) Wildtype Kras2 can inhibit lung carcinogenesis in mice. *Nat. Genet.* **29,** 25–33
32. Wang, Q., Chaerkady, R., Wu, J., Hwang, H. J., Papadopoulos, N., Kopelovich, L., Maitra, A., Matthaei, H., Eshleman, J. R., Hruban, R. H., Kinzler, K. W., Pandey, A., and Vogelstein, B. (2011) Mutant proteins as cancer-specific biomarkers. *Proc. Natl. Acad. Sci.*. **108,** 2444–2449
33. Thery, C., Zitvogel, L., and Amigorena, S. (2002) Exosomes: composition, biogenesis and function. *Nat. Rev. Immunol.* **2,** 569–579
34. Tian, T., Wang, Y., Wang, H., Zhu, Z., and Xiao, Z. (2010) Visualizing of the cellular uptake and intracellular trafficking of exosomes by live-cell microscopy. *J. Cell. Biochem.* **111,** 488–496
35. Gould, S. J., Booth, A. M., and Hildreth, J. E. (2003) The Trojan exosome hypothesis. *Proc. Natl. Acad. Sci.* **100,** 10592–10597
36. Kim, J. B. (2005) Three-dimensional tissue culture models in cancer biology. *Semin. Cancer Biol.* **15,** 365–377
37. Benton, G., George, J., Kleinman, H. K., and Arnaoutova, I. P. (2009) Advancing science and technology via 3D culture on basement membrane matrix. *J. Cell. Physiol.* **221,** 18–25
38. McKay, J., Wang, X., Ding, J., Buss, J. E., and Ambrosio, L. (2011) H-ras resides on clathrin-independent ARF6 vesicles that harbor little RAF-1, but not on clathrin-dependent endosomes. *Biochim. Biophys. Acta* **1813,** 298–307
39. Kofer-Geles, M., Gottfried, I., Haklai, R., Elad-Zefadia, G., Kloog, Y., and Ashery, U. (2009) Rasosomes spread Ras signals from plasma membrane "hotspots." *Biochim. Biophys. Acta* **1793,** 1691–1702
40. Rotblat, B., Yizhar, O., Haklai, R., Ashery, U., and Kloog, Y. (2006) Ras and its signals diffuse through the cell on randomly moving nanoparticles. *Cancer Res.* **66,** 1974–1981
41. Subra, C., Grand, D., Laulagnier, K., Stella, A., Lambeau, G., Paillasse, M., De Medina, P., Monsarrat, B., Perret, B., Silvente-Poirot, S., Poirot, M., and Record, M. (2010) Exosomes account for vesicle-mediated transcellular transport of activatable phospholipases and prostaglandins. *J. Lipid Res.* **51,** 2105–2120
42. Ji, H., Erfani, N., Tauro, B. J., Kapp, E. A., Zhu, H. J., Moritz, R. L., Lim, J. W., and Simpson, R. J. (2008) Difference gel electrophoresis analysis of Ras-transformed fibroblast cell-derived exosomes. *Electrophoresis* **29,** 2660–2671
43. Pisitkun, T., Shen, R. F., and Knepper, M. A. (2004) Identification and proteomic profiling of exosomes in human urine. *Proc. Natl. Acad. Sci.* **101,** 13368–13373
44. Mathivanan, S., Lim, J. W., Tauro, B. J., Ji, H., Moritz, R. L., and Simpson, R. J. (2010) Proteomics analysis of A33 immunoaffinity-purified exosomes released from the human colon tumor cell line LIM1215 reveals a tissue-specific protein signature. *Mol. Cell. Proteomics* **9,** 197–208
45. Ahearn, I. M., Haigis, K., Bar-Sagi, D., and Philips, M. R. (2012) Regulating the regulator: post-translational modification of RAS. *Nat. Rev. Mol. Cell Biol.* **13,** 39–51
46. Sasaki, A. T., Carracedo, A., Locasale, J. W., Anastasiou, D., Takeuchi, K., Kahoud, E. R., Haviv, S., Asara, J. M., Pandolfi, P. P., and Cantley, L. C. (2011) Ubiquitination of K-Ras enhances activation and facilitates binding to select downstream effectors. *Sci. Signal.* **4,** ra13
47. van Niel, G., Porto-Carreiro, I., Simoes, S., and Raposo, G. (2006) Exosomes: a common pathway for a specialized function. *J. Biochem.* **140,** 13–21
48. Kim, W., Bennett, E. J., Huttlin, E. L., Guo, A., Li, J., Possemato, A., Sowa, M. E., Rad, R., Rush, J., Comb, M. J., Harper, J. W., and Gygi, S. P. (2011) Systematic and quantitative assessment of the ubiquitin-modified proteome. *Mol. Cell* **44,** 325–340
49. Nagaraj, N., Wisniewski, J. R., Geiger, T., Cox, J., Kircher, M., Kelso, J., Paabo, S., and Mann, M. (2011) Deep proteome and transcriptome mapping of a human cancer cell line. *Mol. Syst. Biol.* **7,** 548
50. Lee, H. D., Koo, B. H., Kim, Y. H., Jeon, O. H., and Kim, D. S. (2012) Exosome release of ADAM15 and the functional implications of human macrophage-derived ADAM15 exosomes. *FASEB J.* **26,** 3084–3095
51. Nazarenko, I., Rana, S., Baumann, A., McAlear, J., Hellwig, A., Trendelenburg, M., Lochnit, G., Preissner, K. T., and Zoller, M. (2010) Cell surface tetraspanin Tspan8 contributes to molecular pathways of exosome-induced endothelial cell activation. *Cancer Res.* **70,** 1668–1678
52. Simons, M., and Raposo, G. (2009) Exosomes—vesicular carriers for intercellular communication. *Curr. Opin. Cell Biol.* **21,** 575–581
53. Brockbank, E. C., Bridges, J., Marshall, C. J., and Sahai, E. (2005) Integrin beta1 is required for the invasive behaviour but not proliferation of squamous cell carcinoma cells in vivo. *Br. J. Cancer* **92,** 102–112
54. Yan, Z., Chen, M., Perucho, M., and Friedman, E. (1997) Oncogenic Ki-ras but not oncogenic Ha-ras blocks integrin beta1-chain maturation in colon epithelial cells. *J. Biol. Chem.* **272,** 30928–30936
55. Hood, J. D., and Cheresh, D. A. (2002) Role of integrins in cell invasion and migration. *Nat. Rev. Cancer* **2,** 91–100
56. Schramm, K., Krause, K., Bittroff-Leben, A., Goldin-Lang, P., Thiel, E., and Kreuser, E. D. (2000) Activated K-ras is involved in regulation of integrin expression in human colon carcinoma cells. *Int. J. Cancer* **87,** 155–164
57. Dajee, M., Lazarov, M., Zhang, J. Y., Cai, T., Green, C. L., Russell, A. J., Marinkovich, M. P., Tao, S., Lin, Q., Kubo, Y., and Khavari, P. A. (2003) NF-kappaB blockade and oncogenic Ras trigger invasive human epidermal neoplasia. *Nature* **421,** 639–643
58. Chai, H., and Brown, R. E. (2009) Field effect in cancer—an update. *Ann. Clin. Lab. Sci.* **39,** 331–337
59. Richards, J. S., Fan, H. Y., Liu, Z., Tsoi, M., Lague, M. N., Boyer, A., and Boerboom, D. (2011) Either Kras activation or Pten loss similarly enhance the dominant-stable CTNNB1-induced genetic program to promote granulosa cell tumor development in the ovary and testis. *Oncogene*
60. Kataoka, H., Igarashi, H., Kanamori, M., Ihara, M., Wang, J. D., Wang, Y. J., Li, Z. Y., Shimamura, T., Kobayashi, T., Maruyama, K., Nakamura, T., Arai, H., Kajimura, M., Hanai, H., Tanaka, M., and Sugimura, H. (2004) Correlation of EPHA2 overexpression with high microvessel count in human primary colorectal cancer. *Cancer Sci.* **95,** 136–141
61. Piedra, J., Miravet, S., Castano, J., Palmer, H. G., Heisterkamp, N., Garcia de Herreros, A., and Dunach, M. (2003) p120 catenin-associated Fer and Fyn tyrosine kinases regulate beta-catenin Tyr-142 phosphorylation and

beta-catenin-alpha-catenin interaction. *Mol. Cell. Biol.* **23,** 2287–2297
62. Futreal, P. A., Coin, L., Marshall, M., Down, T., Hubbard, T., Wooster, R., Rahman, N., and Stratton, M. R. (2004) A census of human cancer genes. *Nat. Rev. Cancer* **4,** 177–183
63. Slaughter, D. P., Southwick, H. W., and Smejkal, W. (1953) Field cancerization in oral stratified squamous epithelium; clinical implications of multicentric origin. *Cancer* **6,** 963–968
64. Forbes, S. A., Bindal, N., Bamford, S., Cole, C., Kok, C. Y., Beare, D., Jia, M., Shepherd, R., Leung, K., Menzies, A., Teague, J. W., Campbell, P. J., Stratton, M. R., and Futreal, P. A. (2011) COSMIC: mining complete cancer genomes in the Catalogue of Somatic Mutations in Cancer. *Nucleic Acids Res.* **39,** D945-D950
65. Schubbert, S., Shannon, K., and Bollag, G. (2007) Hyperactive Ras in developmental disorders and cancer. *Nat. Rev. Cancer* **7,** 295–308
66. Gross, J. C., Chaudhary, V., Bartscherer, K., and Boutros, M. (2012) Active Wnt proteins are secreted on exosomes. *Nat. Cell Biol.* **14,** 1036–1045
67. Peinado, H., Aleckovic, M., Lavotshkin, S., Matei, I., Costa-Silva, B., Moreno-Bueno, G., Hergueta-Redondo, M., Williams, C., Garcia-Santos, G., Ghajar, C., Nitadori-Hoshino, A., Hoffman, C., Badal, K., Garcia, B. A., Callahan, M. K., Yuan, J., Martins, V. R., Skog, J., Kaplan, R. N., Brady, M. S., Wolchok, J. D., Chapman, P. B., Kang, Y., Bromberg, J., and Lyden, D. (2012) Melanoma exosomes educate bone marrow progenitor cells toward a pro-metastatic phenotype through MET. *Nat. Med.* **18,** 883–891
68. Webber, J., Steadman, R., Mason, M. D., Tabi, Z., and Clayton, A. (2010) Cancer exosomes trigger fibroblast to myofibroblast differentiation. *Cancer Res.* **70,** 9621–9630
69. Paget, S. (1989) The distribution of secondary growths in cancer of the breast. 1889. *Cancer Metastasis Rev.* **8,** 98–101
70. Kaplan, R. N., Riba, R. D., Zacharoulis, S., Bramley, A. H., Vincent, L., Costa, C., MacDonald, D. D., Jin, D. K., Shido, K., Kerns, S. A., Zhu, Z., Hicklin, D., Wu, Y., Port, J. L., Altorki, N., Port, E. R., Ruggero, D., Shmelkov, S. V., Jensen, K. K., Rafii, S., and Lyden, D. (2005) VEGFR1-positive haematopoietic bone marrow progenitors initiate the pre-metastatic niche. *Nature* **438,** 820–827